Mechanisms of elastic enhancement and hindrance for finite length undulatory swimmers in viscoelastic fluids

Becca Thomases and Robert D. Guy

Department of Mathematics, University of California, Davis

(Dated: July 21, 2014)

A computational model of finite-length undulatory swimmers is used to examine the physical origin of the effect of elasticity on swimming speed. We explore two distinct target swimming strokes, one derived from the motion of *C. elegans*, with large head undulations, and a contrasting stroke with large tail undulations. We show that both favorable stroke asymmetry and swimmer elasticity contribute to a speed-up, but a substantial boost results only when these two effects work together. We reproduce conflicting results from the literature simply by changing relevant physical parameters.

Low Reynolds number swimming of microorganisms in Newtonian fluids is an extensively studied classical problem and the underlying physics is well understood [1]. However, many biological fluids such as mucus are mixtures of water and polymers and are more appropriately described as viscoelastic fluids. Recently, there have been many studies on locomotion in complex fluids [2–16]. Both experiments and theory have exhibited that viscoelasticity can lead to either an enhancement or retardation of swimming, but a complete understanding of this problem is lacking. Given the many different types of materials that exhibit viscoelastic properties, and the many different types of small scale organisms, it is unlikely that there is a simple answer to what effects viscoelasticity has on swimming, and subclasses of problems must be considered.

Here we focus on finite-length undulatory swimmers with large-amplitude planar beat in an Oldroyd-B fluid. Asymptotic analysis of infinitely long, small-amplitude swimmers showed that swimming is hindered by the addition of elastic stresses [9]. Numerical simulation of finite-length, large-amplitude swimmers showed that under some conditions, the swimming speed may be enhanced by elasticity [13], with a peak in swimming speed when the relaxation time of the fluid is similar to the period of the undulation. However, experimental measurements of the undulatory motion of *C. elegans* showed that swimming is always slowed with increasing elasticity [14], while an experiment using a physical model of a swimmer showed that swimming speed was an increasing function of the elasticity of the fluid [12].

In this letter we use computational modeling to examine the physical origin of the elastic speed-up/slowdown in finite-length undulatory swimmers. Our data-based model stroke comes from the motion of *C. elegans* [14], whose stroke shows larger undulations at the head. Others have studied strokes with larger undulations at the tail [12, 13]. We contrast these two different types of swimmers and show that stroke asymmetries lead to stress distribution asymmetries which, when fa-

vorable, can contribute to an elastic speed-up. When the swimmer is flexible, the body response to changing fluid stresses provides an additional speed-up. We conclude that a substantial speed-up, like those reported in the literature [12, 13], can only occur when these two effects work together. We reproduce several seemingly conflicting results [12–14], and demonstrate that they are complementary rather than contradictory.

The model. – We model the swimmer as an inextensible flexible sheet of finite length L immersed in a 2D fluid. We describe the undulatory motion of the swimmer by a curvature function of the form

$$\kappa_0(\ell, t) = A(\ell)\cos\bigl(2\pi t/T + \phi(\ell)\bigr), \tag{1}$$

where $\ell \in [0, L]$ is the body coordinate ($\ell = 0$ is the head). We base our model parameters on *C. Elegans* swimming in a Newtonian fluid [14]; by fitting to data, we obtain $L = 1.2$ mm, $T = 0.5$ s, $A(\ell) = 5.3 - 3.1\ell$ mm^{-1}, and $\phi(\ell) = \pi(L - \ell)$ mm^{-1} [27]. Changes in curvature propagate as waves from the head, with the largest curvature amplitude, to the tail. We call this type of swimmer a "burrower," in contrast to swimmers with larger curvature amplitude at the tail, "kickers," such as in [12, 13]. The kicker stroke is related to the burrower stroke by $\kappa_0^{\text{kicker}}(\ell, t) = \kappa_0^{\text{burrower}}(L - \ell, t - t_0)$, where t_0 is a phase shift that keeps the head in phase with the burrower.

We use the immersed boundary method to solve for the coupled motion of the fluid and the swimmer [17]. Both inextensibility and shape are imposed (approximately) by forces that are designed to penalize extension and deviation from a prescribed target curvature. These forces are derived from the variation of bending and extension (stretching) energy functionals. For example, the bending energy is $E_{\text{b}} = k_{\text{b}}/2 \int_\Gamma (\kappa - \kappa_0)^2 \, d\ell$, where k_{b} is the bending stiffness, κ is the curvature of the sheet, and κ_0 is the prescribed target curvature. One can interpret the model as an active sheet with bending stiffness k_{b} driven by an active body moment density $k_{\text{b}}\kappa_0$. We scale forces relative to viscous forces so that for $k_{\text{b}} \gg 1$, the real-

ized shape of the swimmer is very close to the prescribed shape; we call these swimmers *stiff* and use $k_b = 40$ in our simulations. For $k_b \sim 1$, elastic forces and viscous forces are of the same scale and the realized shape is the result of fluid-structure interaction; we use $k_b = 2$ and call these swimmers *soft*.

The viscoelastic fluid is described by the Oldroyd-B model at zero Reynolds number [18], regularized by polymer stress diffusion [19, 20]. The system of equations describing the fluid are

$$\Delta \mathbf{u} - \nabla p + \xi \mathrm{De}^{-1} \nabla \cdot \boldsymbol{\tau} + \mathbf{f} = 0, \text{ and } \nabla \cdot \mathbf{u} = 0, \quad (2)$$

$$\overset{\nabla}{\boldsymbol{\tau}} + \mathrm{De}^{-1}(\boldsymbol{\tau} - \mathbf{I}) = \varepsilon \triangle \boldsymbol{\tau}, \quad (3)$$

where $\mathbf{u}$ is the fluid velocity, p is the pressure, $\boldsymbol{\tau}$ is the viscoelastic stress, and $\mathbf{f}$ is the elastic force density generated by the swimmer. The upper convected time derivative is defined by $\overset{\nabla}{\boldsymbol{\tau}} \equiv \partial \boldsymbol{\tau} / \partial t + \mathbf{u} \cdot \nabla \boldsymbol{\tau} - (\nabla \mathbf{u} \, \boldsymbol{\tau} + \boldsymbol{\tau} \, \nabla \mathbf{u}^T)$. Here ξ is the ratio of polymer to solvent viscosity, $\mathrm{De} = T_p/T_f$ is the ratio of the elastic relaxation time to the characteristic flow time-scale, and $\varepsilon \ll 1$ is the stress diffusion coefficient. Based on the data which defined the burrower stroke, we nondimensionalize with a characteristic length scale of 1 mm, time scale of $T_f = 1$ s, and stress scale μ/T_f, where μ is the viscosity of water. Other model and numerical parameters are given in [28].

Results.– Fig. 1 shows the average Stokes-normalized swimming speed as a function of the Deborah number for soft and stiff kickers and burrowers. The time average is taken over one period after the speed has equilibrated, which we take as the greater of 20 periods or 20 times the relaxation time. For all but the soft kicker, any elasticity tends to slow down the swimmers, consistent with the predictions of [9, 11]. Here we examine what allows the soft kicker to overcome this elastic resistance, and in doing so, we systematically demonstrate how changing fluid elasticity and swimmer elasticity affects swimming speed. From this we gain insight into the local maximum in swimming speed for $\mathrm{De} \sim 1$ (for all but the stiff burrower). Finally we examine the swimming speed slow down for $\mathrm{De} \gtrsim 2$.

First we study the effect of fluid elasticity by looking at the polymer stress induced by the motion of soft kickers and burrowers. We focus on $\mathrm{De} = 1$ to gain insight into the local maxima seen in Fig. 1. Fig. 2 (a) shows the polymer stress energy, computed as the trace of the polymer stress tensor, about the soft kicker and burrower (head on right) at two times during a period for $\mathrm{De} = 1$. Two significant differences between the kicker and burrower stresses are their scales and their spatial distributions. For the kicker, there is a concentration of stress at the tail which persists over the period, whereas for the burrower, the polymer stress concentrates along the entire body of the swimmer and is about 3-4 times smaller at its maximum.
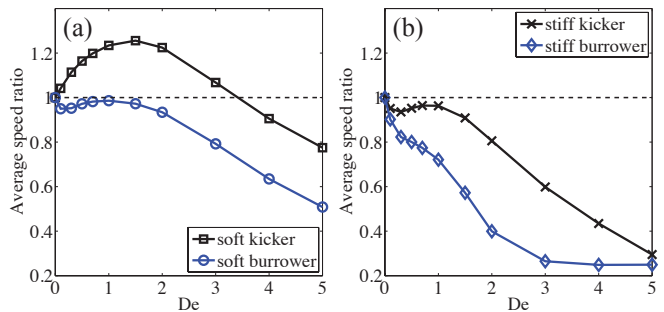

FIG. 1: (a)-(b): The ratio of average swimmer speed to that of the Newtonian swimmer as a function of De, varying stroke type and bending stiffness. (color online)

To analyze the effect these stresses have on motion, we look at the swimmer horizontal center-of-mass position over one period shown in Fig. 2 (b)-(c). With no elasticity ($\mathrm{De} = 0$) we see major differences in the translational locomotion inherent to the kicker versus burrower stroke. In particular, burrowers swim faster than kickers because there is little to no recoil over the cycle of the stroke, whereas kickers lose about 25% of progression to recoil. Elasticity effects both progression and recoil but in different ways for kicker and burrower, due to the different stress distributions for these strokes.

For the kicker, elasticity ($0 < \mathrm{De} \lesssim 3$) enhances progression by as much as 20%, while recoil remains nearly constant. The onset of enhanced progression for the $\mathrm{De} = 1$ kicker coincides with a local maxima in the average back stress (average stress to the left of the center of mass), see Fig. 2 (a) (i). In other words, when the back stress is greatest the swimmer moves forward. Similarly when the front stress is greatest, the swimmer begins to recoil (Fig. 2 (a) (ii)). The local maxima of back and front stress are noted on Fig. 2 (b) (and (c)) with squares and circles, respectively. The average back stress is more than 5 times as large as the average front stress, and we see an enhancement to progression as if the swimmer is "kicking off" of the accumulated stresses. In [13] the authors conjectured that the region of highly strained fluid at the tail restricts backward slippage contributing to an increase in speed. While we do see backward slippage, it appears to be nearly constant as elasticity changes.

Like the kicker, the burrower's back stress is maximized at the beginning of progression (Fig. 2 (a) (iii)) and the front stress is maximized at the beginning of recoil (Fig. 2 (a) (iv)). Unlike the kicker, we see enhanced recoil as if the accumulated front stress must be "burrowed through". The differing response may be due to the fact that for the burrower the polymer stress is distributed much more evenly around the body, and in particular, the burrower has, on average, half as much back stress and twice as much front stress as the kicker.
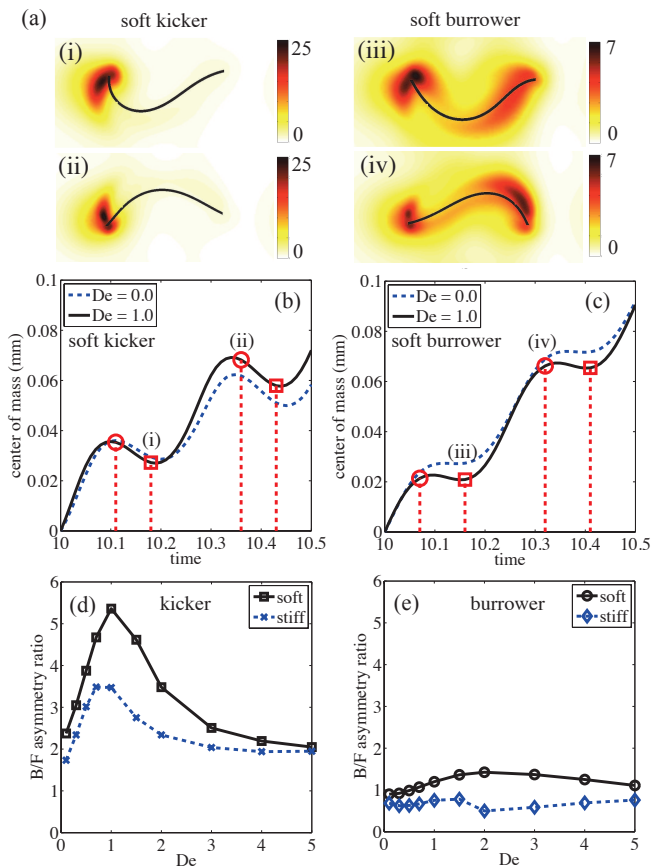
Now turning to both soft and stiff swimmers at all

FIG. 2: (a) Contour plots of the polymer stress energy at two times during a period for De = 1, (i)-(ii) soft kicker, (iii)-(iv) soft burrower (head on right). (b)-(c): The location of the horizontal component of the swimmer center of mass is plotted over one period at $t = 10$ for De = 0, 1; markers correspond to local maxima in front (circles) and back (squares) stress. (d)-(e): Back-front stress asymmetry ratio (time-averaged ratio of back stress to front stress) for $0 \leq De \leq 5$. (color online)

De, we utilize this back-front asymmetry in stresses to quantify an "asymmetry ratio," the time-averaged ratio of back stress to front stress, plotted in Fig. 2 (d) - (e). We see that the kickers overall have high (≥ 2) asymmetry ratios which reach a maximum around De ~ 1. This back-front asymmetry maximum correlates well with the maximum in swimming speed for kickers seen in Fig. 1 (a), and likely contributes to the speed boost seen for De ~ 1. For burrowers this ratio is close to one for all De. This is consistent with the fact that the burrowers do not see a speed boost. For both kickers and burrowers this ratio decreases as the swimmer goes from soft to stiff. The stiff kicker retains the De ~ 1 local maxima, and though decreased, it is still greater than 3. The stiff burrower meanwhile always has a ratio less than 1 meaning there is more front stress than back. Fluid elasticity contributes to a speed boost when there is a high asymmetry ratio, but this measure alone does not explain the local maximum in speed ratio at De ~ 1 for the soft bur-

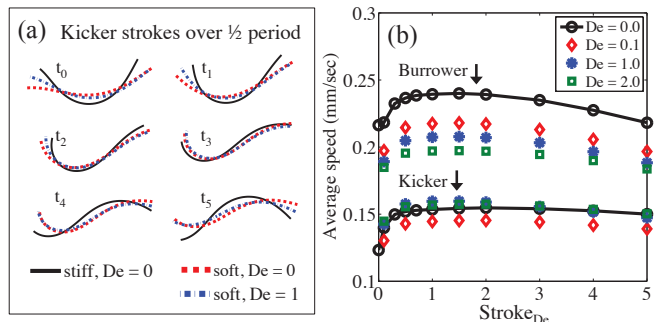rower nor the slow down at large De. Next we look at how swimmer elasticity effects the swimming speed.

FIG. 3: (a) Kicker shapes at times evenly spaced within a half-period: stiff at De = 0, soft at De = 0, 1. (b) Non-normalized average speed for stiff kicker and burrower for different De (see markers) as a function of $Stroke_{De}$, where changes in this parameter correspond with passive dynamic stroke changes for soft swimmers indexed by De. (color online)

The viscoelastic boost for soft kickers depends crucially on the elasticity of the swimmer and there are significant deviations between target and achieved curvatures, varying with De, that can be as large as 40%. For the stiff kicker deviations are at most 3%. Fig. 3 (a) shows the kinematics of the swimmer body over a half-period for a stiff kicker in a Newtonian fluid (De = 0) and soft kickers at De = 0, 1. The stiff and soft strokes are noticeably different, and the addition of elasticity tends to return the stroke towards the more favorable stroke of the stiff swimmer [29].

To isolate the effect of passive dynamics for soft swimmers we index the stroke changes with De by fitting each soft swimmer's curvature deviation to the solution of the equation that describes a freely vibrating beam and use the first 4 modes to capture these deviations. We then prescribe this idealized curvature as the target curvature for a stiff swimmer, and the so-called $Stroke_{De}$ is the parameter referring to the stroke change. Fig. 3 (b) (solid curve) shows the non-normalized swimming speed for a stiff kicker and burrower, in a Newtonian fluid, as a function of this stroke parameter. Both the kicker and burrower show dramatic speed-ups of 25% and 10%, respectively, as a functions of stroke changes alone with maxima coming from the De = 1 soft swimmer.

Fig. 3 (b) also shows how the swimming speed depends on $Stroke_{De}$ when elasticity is added to the fluid (De = 0.1, 1.0, 2.0). The kicker shows a non-monotonic response to elasticity; a small amount of elasticity (De = 0.1) does not boost the swimming speed but with De = 1, 2 there is a fluid elasticity boost, strongest at $Stroke_{De} \sim 1$ and De ~ 1 which diminishes for higher $Stroke_{De}$ and De. For the burrower, fluid elasticity monotonically hinders swimming speed.

With this additional information we can revisit Fig.

1 and examine the local maxima. For the soft kicker, stroke changes induced by passive dynamics boost the swimming speed and the high back-front asymmetry ratio indicates a boost from fluid elasticity as well. Both of these boosts are largest at De ~ 1. Thus the soft kicker has a "double-boost", which may be necessary to get an advantage from elasticity. The soft burrower gets a boost from the passive dynamics, also largest at De ~ 1, but does not get a boost from the fluid elasticity. A cancellation of these effects leads to a nearly constant speed for small De with a slight peak at De $= 1$. The stiff kicker sees no advantage from passive dynamics (as the stroke is very close to the prescribed stroke) but does get a boost from the back-front asymmetry of elastic stress (again largest at De ~ 1). This single boost also leads to a nearly constant speed for small De with a peak at De $= 1$. Finally, the stiff burrower has neither boost and we see a monotonically decreasing swimming speed as a function of De. With this explanation of the low De behavior of the speed ratio we next consider the large De effect.
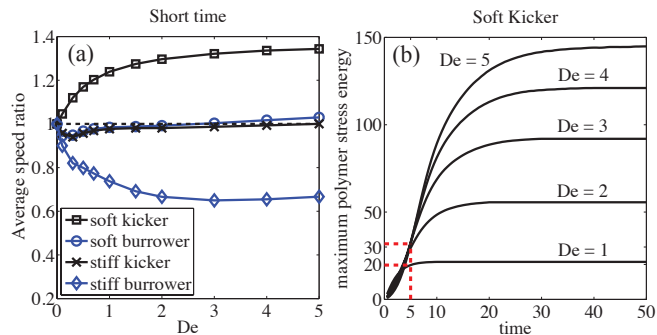

FIG. 4: (a): The ratio of average swimmer speed to that of the Newtonian swimmer as a function of De, varying stroke type, bending stiffness on a short time scale. (b) Time evolution of maximum polymer stress energy for $1 \leq \text{De} \leq 5$, soft kicker. (color online)

Fig. 1 shows that for De ≥ 2, for all swimmers, the swimming speed is monotonically decreasing. We can remove this large De effect by looking at a short time-scale. We take the average of the swimming speed after 10 periods, at which time the speed has effectively equilibrated for De ≤ 1, but is still changing for larger De. Fig. 4 (a) shows the average speed ratio as a function of De when the average is taken at this short time-scale. The swimming speed is monotonically increasing in De for soft kickers. Soft burrowers and stiff kickers have near constant swimming speeds on short-time scales, while stiff burrowers are slowed substantially.

On short time-scales there is little change in the size of the polymer stress, the asymmetry ratio, and the passive dynamic stroke changes over $1 \leq \text{De} \leq 5$ (data not shown). These results imply that the early elastic effects come from the passive dynamic stroke changes and the polymer stress asymmetries. In Fig. 4 (b) we show the evolution of the maximum of the polymer stress energy, and at short times the size of the stress is similar for $1 \leq \text{De} \leq 5$, but there is a 600% increase in stress from De $= 1$ to De $= 5$ at equilibrium (similar results hold for the soft burrower). For stiff swimmers, the maximum stress energy grows on the same time scale, although it is between 2 (at De $= 1$) and 6 (at De $= 5$) times larger overall. The increased resistance from these large elastic stresses that develop on long time-scales swamps any advantage gained from initial asymmetries in fluid elasticity, or passive dynamic stroke changes, hindering swimming speed for large De.

Discussion.– Our model of finite-length undulatory swimmers shows that while swimming speed depends on the type of stroke it also depends sensitively on both fluid elasticity and swimmer elasticity. While fluid elasticity generically slows swimmers down, a speed boost can be gained for soft swimmers from passive dynamic stroke changes and for kickers from favorable asymmetries in the polymer stress distribution. Soft kickers get both boosts which results in a viscoelastic speed-up. With only one boost, stiff kickers and soft burrowers are always hindered by fluid elasticity but only slightly for small De. Large elastic stresses which develop on long time-scales for large De slow down swimmers.

We have presented elastic speed-up results for a single curvature gradient with a fixed amount of body elasticity. By changing these two parameters one can obtain different percent elastic speed-ups (well beyond 25%) with local maxima occurring at a range of De. In fact for certain parameters we see speed-up beyond De $= 5$, consistent with the results reported in [12]. Returning to the other conflicting results of [13] and [14], the stroke used here is based on the data from [14], and we are able to recover the results from [13] by simply changing the direction of the wave. We note that although our Deborah number is defined slightly differently from [13], there is no significance to the specific value of De where the speed-up is maximized, because it depends sensitively on the curvature gradient and the stiffness parameter.

In the model presented here, body stiffness and applied active moments are both proportional to the body stiffness parameter k_{b}. Alternately, one could change the body stiffness and strength of driving moments independently to isolate their effects on the resulting stroke. Real biological systems are much more complicated in that the driving forces change in response to mechanical, neurological, or chemical feedback from the environment. For example, hyperactivated spermatozoan cells exhibit very different flagellar waveforms and swimming kinematics than nonactivated cells [21]. Hyperactivation results in slower swimming in Newtonian fluids, but faster swimming in viscoelastic fluids [22], and it is essential to fertilization [23].

There are similarities between our results and those

for helical swimmers. Like undulatory swimmers, asymptotics show that small pitch angle helical swimmers are hindered by elasticity [8], but for sufficiently large angle, fluid elasticity can increase the swimming speed with a peak near De ~ 1 [2, 15]. Unlike undulatory swimmers, the speed-up was observed for infinitely long swimmers. In [15], they observed stress asymmetries in the angular direction that appear related to the elastic speed-up/slow-down, consistent with our observation of the role of the back-front stress asymmetry.We note that the size of the boost observed in physical experiments [2] was substantially greater than in the theoretical result of a rigid helix [15]. Our results indicate that a passive elastic response of the body can provide a significant additional boost, and this may also be the case for helical swimmers, but to our knowledge this has not been studied.

---

[1] E. Lauga and T. Powers, Rep. Prog. Phys. **72**, 096601 (2009).

[2] B. Liu, T. R. Powers, and K. S. Breuer, Proceedings of the National Academy of Sciences **108**, 19516 (2011).

[3] L. Zhu, E. Lauga, and L. Brandt, Physics of Fluids (1994-present) **24**, 051902 (2012).

[4] N. C. Keim, M. Garcia, and P. E. Arratia, Physics of Fluids (1994-present) **24**, 081703 (2012).

[5] T. Normand and E. Lauga, Physical Review E **78**, 061907 (2008).

[6] H. C. Fu, V. B. Shenoy, and T. R. Powers, EPL (Europhysics Letters) **91**, 24002 (2010).

[7] T. D. Montenegro-Johnson, D. J. Smith, and D. Loghin, Physics of Fluids (1994-present) **25**, 081903 (2013).

[8] H. C. Fu, C. W. Wolgemuth, and T. R. Powers, Physics of Fluids (1994-present) **21**, 033102 (2009).

[9] E. Lauga, Physics of Fluids (1994-present) **19**, 083104 (2007).

[10] M. Dasgupta, B. Liu, H. C. Fu, M. Berhanu, K. S. Breuer, T. R. Powers, and A. Kudrolli, Physical Review E **87**, 013015 (2013).

[11] H. C. Fu, T. R. Powers, and C. W. Wolgemuth, Physical review letters **99**, 258101 (2007).

[12] J. Espinosa-Garcia, E. Lauga, and R. Zenit, Physics of Fluids (1994-present) **25**, 031701 (2013).

[13] J. Teran, L. Fauci, and M. Shelley, Physical review letters **104**, 038101 (2010).

[14] X. N. Shen and P. E. Arratia, Physical review letters **106**, 208101 (2011).

[15] S. E. Spagnolie, B. Liu, and T. R. Powers, Physical review letters **111**, 068101 (2013).

[16] A. M. Leshansky, Phys. Rev. E **80**, 051911 (2009).

[17] L. J. Fauci and C. S. Peskin, Journal of Computational Physics **77**, 85 (1988).

[18] R. B. Bird, O. Hassager, R. Armstrong, and C. Curtiss, *Dynamics of Polymeric Liquids, Vol. 2: Kinetic Theory* (John Wiley and Sons, 1980).

[19] R. Sureshkumar and A. N. Beris, Journal of Non-Newtonian Fluid Mechanics **60**, 53 (1995).

[20] B. Thomases, J. Non-Newt. Fluid Mech **166**, 1221 (2011).

[21] S. S. Suarez, Human Reproduction Update **14**, 647 (2008).

[22] S. S. Suarez and X. Dai, Biology of Reproduction **46**, 686 (1992).

[23] T. A. Quill, S. A. Sugden, K. L. Rossi, L. K. Doolittle, R. E. Hammer, and D. L. Garbers, Proceedings of the National Academy of Sciences **100**, 14869 (2003).

[24] J. M. Rallison and E. J. Hinch, J. of Non-Newt Fluid Mech. **29**, 37 (1988).

[25] M. Renardy, J. of Non-Newt Fluid Mech. **138**, 204 (2006).

[26] B. Thomases and M. Shelley, Phys. Fluids **19**, 103103 (2007).

[27] Data provided by Paulo Arratia and Xiaoning Shen.

[28] The system is solved in a 2D periodic domain of size $[0,2] \times [0,1]$, with $dt = 10^{-3}$, and $dx = 2^{-7}$. We fix $\xi = 0.5$, consistent with [13], and $\varepsilon = 0.01$ which provides a regularization of the equation to control large polymer stress gradient growth [20, 24–26].We enforce inextensibility with a dimensionless stiffness constant of 2500.

[29] For De $\lesssim 4$ stiff kickers swim up to twice as fast as soft kickers.